Compression Induced Folding of a Sheet: An Integrable System

Haim Diamant and Thomas A. Witten

Phys. Rev. Lett. **107**, 164302 — Published 11 October 2011

DOI: 10.1103/PhysRevLett.107.164302

Compression Induced Folding of a Sheet: An Integrable System

Haim Diamant*
Raymond & Beverly Sackler School of Chemistry, Tel Aviv University, Tel Aviv 69978, Israel

Thomas A. Witten†
Department of Physics and James Franck Institute, University of Chicago, Chicago, Illinois 60637, USA

The apparently intractable shape of a fold in a compressed elastic film lying on a fluid substrate is found to have an exact solution. Such systems buckle at a nonzero wavevector set by the bending stiffness of the film and the weight of the substrate fluid. Our solution describes the entire progression from a weakly displaced sinusoidal buckling to a single large fold that contacts itself. The pressure decrease is exactly quadratic in the lateral displacement. We identify a complex wavevector whose magnitude remains invariant with compression.

PACS numbers: 46.32.+x 46.70.-p 68.60.Bs 81.16.Rf

Composite structures, containing a fluid substrate covered by a thin rigid layer, are commonly found in biological tissues and synthetic coatings. Unlike a freely suspended sheet, a supported layer has an intrinsic length scale arising from the competition of bending and substrate energy. Thus, e.g., a compressed sheet floating on a fluid buckles at a wavelength $\lambda = 2\pi[B/(\rho g)]^{1/4}$, B being the bending stiffness, ρ the fluid mass density and g the gravitational acceleration [1–8]. An analogous argument holds for an elastic foundation [9].

In the elastic case, it has long been recognized that this extended periodic wrinkling is always unstable against localized folding for a sufficiently large system [10–14]. With a fluid substrate the same instability obtains [15–19]. Such fold localization has been observed in diverse fluid-supported films — from monolayers and trilayers of nanometer-sized gold particles [15, 16], through submicron-thick polymer films [17], to 10-μm-thick plastic sheets [15]. It has been suggested that the localized folds, observed in certain surfactant monolayers at the water–air interface upon sufficiently fast compression (albeit apparently without prior wrinkling) [20–25], and believed to be important for the function of lungs [26], may be a manifestation of the same phenomenon [15, 18].

The shape of the fold beyond infinitesimal amplitude has only been known numerically [15, 18]. The numerical studies showed puzzling regularities. For example, the surface pressure appeared to vary exactly quadratically with the displacement. Here we account for these regularities by solving the nonlinear equation for the fold shape exactly. This allows a much deeper analysis of the phenomenon, including its large-deformation limit and the point of self-contact, which are central to the folding observed in experiments. In a broader context, the current work adds an item to the precious collection of exactly solvable nonlinear physical problems.

Consider a thin incompressible elastic sheet of length L, width W, and bending modulus B. The sheet is uniaxially compressed along the x direction and assumed to deform in the xz plane while remaining uniform along the y direction; see Fig. 1. Due to incompressibility, the configuration of the sheet is completely defined by the profile of the angle, $\phi(s)$, that the local tangent to the sheet makes with the x axis at arclength s. Alternatively, we can define a height profile, $h(s)$, where $\dot{h} = \sin\phi$ (the dot denoting an s-derivative). The region $z < h$ is occupied by a fluid of mass density $\rho = K/g$. We focus here on localized deformations, and therefore let $L \to \infty$ and set $\phi = \dot{\phi} = h = 0$ at $s \to \pm\infty$.

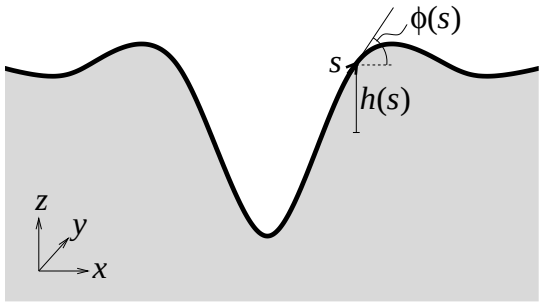

FIG. 1: Schematic view of the system and its parametrization.

The energy $E = E_\mathrm{b} + E_\mathrm{s}$ contains contributions from bending, $E_\mathrm{b} = (WB/2)\int_{-\infty}^{\infty} ds\dot{\phi}^2$, and from the substrate energy, $E_\mathrm{s} = (WK/2)\int_{-\infty}^{\infty} dsh^2\cos\phi$. The displacement along the direction of compression is

$$\Delta = \int_{-\infty}^{\infty} ds(1-\cos\phi), \tag{1}$$

and is related to the pressure by $P = dE/d\Delta$. For brevity we use hereafter units where $B = K = 1$, i.e., we rescale energy by B and length by $(B/K)^{1/4}$, and also let $W = 1$. The pressure P is scaled by $(BK)^{1/2}$.

Invoking a dynamical analogy where s stands for time, we look for the stable configuration by minimizing the

action $\mathcal{S}=\int_{-\infty}^{\infty} ds\mathcal{L}(\phi,h,\dot{\phi},\dot{h})$,

$$\mathcal{L}=\frac{1}{2}\dot{\phi}^2+\frac{1}{2}h^2\cos\phi-P(1-\cos\phi)-Q(s)(\sin\phi-\dot{h}), \quad (2)$$

where P and $Q(s)$ are Lagrange multipliers replacing, respectively, the global constraint on Δ [Eq. (1)] and the local one on the relation between h and ϕ. (In the case of an elastic foundation, the hydrostatic $(h^2/2)\cos\phi$ term is replaced by $h^2/2$ [9].) We identify the conjugate momenta as $p_\phi=\partial\mathcal{L}/\partial\dot{\phi}=\dot{\phi}$ and $p_h=\partial\mathcal{L}/\partial\dot{h}=Q$, and use them to obtain the Hamiltonian, $\mathcal{H}=p_\phi\dot{\phi}+p_h\dot{h}-\mathcal{L}$. Since $\mathcal{L}$ has no explicit dependence on s (the sheet is translation-invariant), $\mathcal{H}$ is a constant of motion,

$$\mathcal{H}=\frac{1}{2}p_\phi^2+p_h\sin\phi-\frac{1}{2}h^2\cos\phi+P(1-\cos\phi)=0, \quad (3)$$

where the last equality follows from the boundary conditions at $s\to\pm\infty$. Equation (3) has the consequence that, wherever the sheet is horizontal ($\phi=0$), we have $|p_\phi|=|h|$, which leads to the geometrical constraint,

$$\phi=0: \quad |\dot{\phi}|=|h|=|\ddot{h}|. \quad (4)$$

Hamilton's equation, $\dot{p}_\phi=-\partial\mathcal{H}/\partial\phi$, yields the following equation of motion:

$$\ddot{\phi}+(h^2/2+P)\sin\phi+p_h\cos\phi=0. \quad (5)$$

Eliminating p_h from Eqs. (3) and (5) and differentiating the resulting equation with respect to s, we get

$$\dddot{\phi}+(\dot{\phi}^2/2+P)\dot{\phi}+h=0. \quad (6)$$

Equation (6) coincides with Euler's *elastica* problem [9, 27, 28]. It expresses the balance of normal forces on an infinitesimal section of the sheet. The last term, which usually corresponds to an external normal force [27], arises here from hydrostatic pressure. Another differentiation yields the equation in terms of ϕ alone,

$$\ddddot{\phi}+[(3/2)\dot{\phi}^2+P]\ddot{\phi}+\sin\phi=0. \quad (7)$$

Continuing to assume that ϕ and its derivatives vanish at infinity, we integrate Eq. (7) once to get

$$\dddot{\phi}\dot{\phi}-\frac{1}{2}\ddot{\phi}^2+\frac{3}{8}\dot{\phi}^4+\frac{1}{2}P\dot{\phi}^2+1-\cos\phi=0. \quad (8)$$

At first glance, the nonlinear Eq. (8) does not seem likely to lend itself to a closed-form solution. Inspection of the equations above reveals, on the other hand, that they readily yield the profile and all of its derivatives at $s=0$. Let us specialize, for instance, to a symmetric deformation about a downward-pointing fold at the origin [as in Fig. 2(a)], where $\phi(0)=\ddot{\phi}(0)=0$. We can then apply Eqs. (6) and (8) at $s=0$ and, thanks to the geometrical condition of Eq. (4), solve for $\dot{\phi}(0)$ and $\dddot{\phi}(0)$,

$$\dot{\phi}(0)=-h(0)=2(2-P)^{1/2}, \quad (9)$$

and $\dddot{\phi}(0)=-2(3-P)(2-P)^{1/2}$. Higher derivatives are obtained from Eq. (7) and its successive differentiation. The complete knowledge of the power-series at $s=0$ hints that the problem may be integrable.

Another indication is suggested by the integrable physical-pendulum (PP) equation, $\ddot{\phi}+q^2\sin\phi=0$, whose solutions are

$$\phi(s)=\pm4\tan^{-1}(Ae^{\pm iqs}), \quad (10)$$

for any q and A. It is straightforward to show, by integrating the PP equation once and differentiating it twice, that any of its solutions also solves Eq. (7) for $P=q^2+q^{-2}+c$, where c is an integration constant (set hereafter to zero). Thus, Eq. (10) gives complex solutions to Eq. (8), with the specific complex wavevectors,

$$q=\pm k\pm i\kappa, \quad k=\frac{1}{2}(2+P)^{1/2}, \ \kappa=\frac{1}{2}(2-P)^{1/2}, \quad (11)$$

and an arbitrary amplitude A (the latter following from translation invariance). We note that $k^2+\kappa^2=1$, independent of P, while $k^2-\kappa^2=P/2$. These solutions resemble the 'kink' solutions of the sine-Gordon (SG) equation [29, 30], albeit in the complex plane. When linearized, they coincide with the 'evanescent wave' profile, which can be stabilized adjacent to a boundary for P close to the critical pressure P_c [18].

These findings indicate that Eq. (7) might belong to a hierarchy of integrable nonlinear equations [30, 31], in which the PP equation is a lower-order member. A known hierarchy of equations, referred to as the stationary-sine-Gordon-modified-Korteweg-de-Vries hierarchy [31], indeed contains the stationary SG equation, the PP equation, and Eq. (7) as the first, second, and third members, respectively. To our knowledge, equations in this hierarchy beyond the PP equation have not been linked before to physical phenomena.

To construct localized real solutions out of the complex ones given in Eq. (10), we borrow a scheme from the SG problem. In 'light-cone' coordinates $[u=(x+t)/2, v=(x-t)/2]$, the SG equation, $\partial_{xx}\phi-\partial_{tt}\phi=\partial_{uv}\phi=\sin\phi$, is invariant to the scaling $u\to qu, v\to v/q$ by an arbitrary scale factor q. Given three known solutions of this equation, ϕ_j $(j=0,1,2)$, one can construct another solution, ϕ_3, using the implicit 'ladder' rule [30], $\tan[(\phi_3-\phi_0)/4]=[(q_1+q_2)/(q_1-q_2)]\tan[(\phi_1-\phi_2)/4]$, where q_1 and q_2 are arbitrary scale factors for ϕ_1 and ϕ_2. We attempt the same procedure while substituting for q_1 and q_2 two of the specific P-dependent wavevectors found in Eq. (11). Choosing $\phi_0=0$, $\phi_1=4\tan^{-1}(e^{iq_1s})$, and $\phi_2=4\tan^{-1}(e^{iq_2s})$, with $q_1=k-i\kappa$ and $q_2=-k-i\kappa$, we obtain the odd function $\tan(\phi_3/4)=(\kappa/k)\sin(ks)/\cosh(\kappa s)$. Using instead $\tan(\phi_1/4)=ie^{iq_1s}$ and $\tan(\phi_2/4)=-ie^{iq_2s}$, we get the even counterpart. Substitution of these two functions in Eq. (8) confirms that they indeed solve it exactly. Thus, the following are

exact localized shapes of the angular profile:

$$\text{symmetric fold:}\ \ \phi(s) = 4\tan^{-1}\left[\frac{\kappa\sin(ks)}{k\cosh(\kappa s)}\right]$$
$$\text{antisymmetric fold:}\ \ \phi(s) = 4\tan^{-1}\left[\frac{\kappa\cos(ks)}{k\cosh(\kappa s)}\right]. \quad (12)$$

These functions match the 'breather' solutions of the SG equation [29] when those are projected onto the light cone, $(s = x = t = u, v = 0)$. Due to the symmetries under reflection about the z axis, reflection about the s (or x) axis, and translation along s, the functions $\pm\phi(\pm s + s_0)$, where $\phi(s)$ is either one of the functions in Eq. (12) and s_0 an arbitrary constant, are solutions as well. The existence of odd and even solutions then follows from the aforementioned ladder rule.

Evidently, the equations simplify when κ becomes small, as $P \to P_c = 2$; then, e.g., the symmetric fold has $\phi \simeq 4\kappa \sin s/\cosh(\kappa s)$, which itself is vanishingly small. This is the regime of incipient buckling discussed previously [1, 2, 5, 18, 19]. The buckling is always localized, but the localization length diverges as the threshold is approached [18, 19].

The solution implies very simple relations among the pressure P, the displacement Δ, the central height $|h(0)|$, and the energies. The decay parameter is exactly linear in the displacement, $\kappa = \Delta/8$. Indeed, the expressions for k and κ [Eq. (11)] exactly match the complex wavevector obtained from a linear analysis of the 'evanescent-wave' for $P \to P_c$ [18]. Consequently, the pressure is exactly quadratic in Δ: $P = 2 - \Delta^2/16$, as previously deduced in that limit [18]. The maximum amplitude of a symmetric deformation is $|h(0)| = \Delta/2$. The bending and substrate contributions to the energy are $E_b = \Delta$ and $E_s = \Delta(1 - \Delta^2/48)$. We note that the energies and pressures are identical for the symmetric and antisymmetric cases.

Figure 2 shows the progression of the symmetric and antisymmetric folds as the lateral displacement increases and the pressure decreases. The configurations have been calculated from Eq. (12) according to the parametrization: $x(s) = \int_0^s ds' \cos\phi(s')$, $z(s) = h(0) + \int_0^s ds' \sin\phi(s')$, where $h(0)$ is given for the symmetric fold by Eq. (9) and for the antisymmetric one by $h(0) = 0$.

The symmetric fold is found to contact itself at a small positive pressure, $P \simeq 0.040$ (corresponding to $\Delta \simeq 5.6 \simeq 0.89\lambda$). Self-contact of the antisymmetric fold, by contrast, requires a substantial negative pressure (i.e., tension) of $P \simeq -0.70$ ($\Delta \simeq 6.6 \simeq 1.05\lambda$). Thus, in the case of an antisymmetric configuration the stress in the sheet vanishes prior to self-contact. One can examine the solutions also beyond self-contact, where they produce self-intersecting configurations which are unphysical for a sheet. In particular, at $P = -2$ the oscillations in ϕ disappear. These configurations are shown in Fig. 3.

These remarkably simple yet exact results are consequences of the high level of symmetry characteristic of integrable nonlinear problems [30]. The case of an elastic foundation [10] is physically less simple, since in-plane shear forces (and not merely normal hydrostatic ones) are exerted on the sheet. Although this problem is found to obey the same constraint at extrema [Eq. (4)], it does not exhibit the regularities described above.

The solution presented here provides precise knowledge of shapes and energies in a large class of wrinkling and folding systems. It enables a new means for making precise force actuators and transducers on any scale where uniform, thin sheets can be made, for example. The solution improves the prospects for understanding the unstable motion resulting from folding [23–25] and the observed buckling of nanoparticle monolayers into trilayers [16]. At the molecular scale, it provides a starting point for quantifying the effects of compressibility and self-attraction of surfactant monolayers, as well as the influence of non-fluid aspects of the substrate. More basically, compression-induced folding appears to be a previously unrecognized integrable solitary wave phenomenon, like the sine-Gordon chain and the Korteweg-de Vries hydrodynamic soliton. The results above may be used to construct more complex, multiple-fold shapes. The fundamental reason for the integrability of the problem remains to be understood. It is to be hoped that this understanding will reveal a broader class of physical systems which are integrable for the same reason.

We are indebted to Enrique Cerda for communicating early hints of simple features in this system, and to Ilya Gruzberg for insightful discussions and for recognizing our system as a member of a known hierarchy of integrable systems. We thank Benny Davidovitch and Leo Kadanoff for helpful discussions. We thank the Aspen Center for Physics for its hospitality during part of this work. The research was supported in part by the US–Israel Binational Science Foundation under Grant Number 2006076, and in part by the National Science Foundation's MRSEC Program under Award Number DMR 0820054.

* Electronic address: hdiamant@tau.ac.il
† Electronic address: t-witten@uchicago.edu

[1] S. T. Milner, J.-F. Joanny, and P. Pincus, Europhys. Lett. **9**, 495 (1989).
[2] E. Cerda and L. Mahadevan, Phys. Rev. Lett. **90**, 074302 (2003).
[3] D. Vella, P. Aussillous, and L. Mahadevan, Europhys. Lett. **68**, 212 (2004).
[4] J. Huang, M. Juszkiewicz, W. H. de Jeu, E. Cerda, T. Emrick, N. Menon, and T. P. Russell, Science **317**, 650 (2007).
[5] Q. Zhang and T. A. Witten, Phys. Rev. E **76**, 041608 (2007).
[6] B. Davidovitch, Phys. Rev. E **80**, 025202 (2009).
[7] J. Huang, B. Davidovitch, C. D. Santangelo, T. P. Rus-

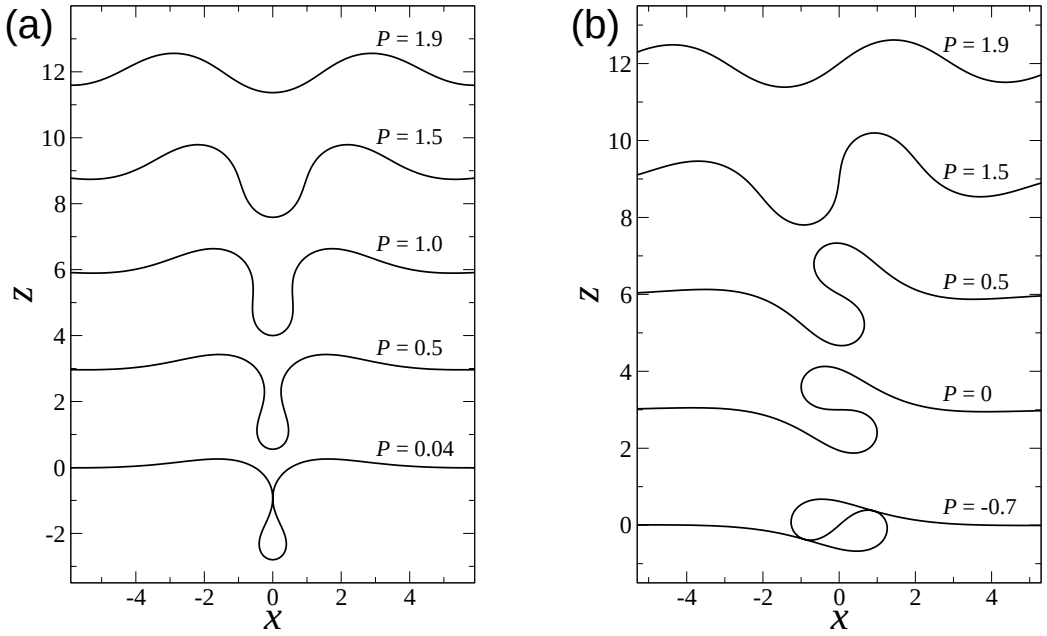

FIG. 2: Symmetric (a) and antisymmetric (b) configurations of the sheet in the xz plane as a function of decreasing pressure (increasing displacement) from a point close to the instability threshold ($P_c = 2$) down to self-contact. The curves are vertically shifted by 3 from one another for clarity.

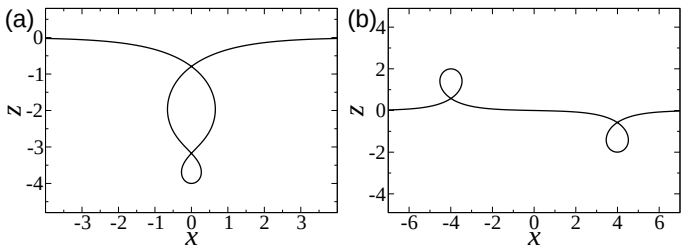

FIG. 3: The fully 'damped' self-intersecting configurations obtained for $P \to -2$. (a) Symmetric configuration for $P = -2$ [$\phi(s) = 4\tan^{-1}(s/\cosh s)$]. (b) Antisymmetric configuration for $P = -1.9999$; as $P \to -2$ the two loops are pushed toward the boundaries, leaving a flat sheet ($\phi = 2\pi$) in between.

sell, and N. Menon, Phys. Rev. Lett. **105**, 038302 (2010).
[8] D. Vella, M. Adda-Bedia, and E. Cerda, Soft Matter **6**, 5778 (2010).
[9] J. M. T. Thompson and G. W. Hunt, *A General Theory of Elastic Stability* (Wiley, London, 1973).
[10] G. W. Hunt, M. K. Wadee, and N. Shiacolas, J. Appl. Mech. **60**, 1033 (1993).
[11] S. H. Lee and A. M. Waas, Int. J. Non-Linear Mech. **31**, 313 (1996).
[12] B. Audoly and A. Boudaoud, J. Mech. Phys. Solids **56**, 2401 (2008).
[13] P. M. Reis, F. Corson, A. Boudaoud, and B. Roman, Phys. Rev. Lett. **103**, 045501 (2009).
[14] F. Brau, H. Vandeparre, A. Sabbah, C. Poulard, A. Boudaoud, and P. Damman, Nat. Phys. **7**, 56 (2011).
[15] L. Pocivavsek, R. Dellsy, A. Kern, S. Johnson, B. Lin, K. Y. C. Lee, and E. Cerda, Science **320**, 912 (2008).
[16] B. D. Leahy, L. Pocivavsek, M. Meron, K. L. Lam, D. Salas, P. J. Viccaro, K. Y. C. Lee, and B. Lin, Phys. Rev. Lett. **105**, 058301 (2010).
[17] D. P. Holmes and A. J. Crosby, Phys. Rev. Lett. **105**, 038303 (2010).
[18] H. Diamant and T. A. Witten, arXiv:1009.2487.
[19] B. Audoly, Phys. Rev. E **84**, 011605 (2011).
[20] M. M. Lipp, K. Y. C. Lee, D. Y. Takamoto, J. A. Zasadzinski, and A. J. Waring, Phys. Rev. Lett. **81**, 1650 (1998).
[21] A. Gopal and K. Y. C. Lee, J. Phys. Chem. B **105**, 10348 (2001).
[22] C. Ybert, W. Lu, G. Möller and C. M. Knobler, J. Phys. Chem. B **106**, 2004 (2002).
[23] Y. Zhang and T. M. Fischer, J. Phys. Chem. B **109**, 3442 (2005).
[24] A. Gopal, V. Belyi, H. Diamant, T. A. Witten, K. Y. C. Lee, J. Phys. Chem. B **110**, 10220 (2006).
[25] M. M. Lozano and M. L. Longo, Langmuir **25**, 3705 (2009).
[26] K. Y. C. Lee, Ann. Rev. Phys. Chem. **59**, 771 (2008).
[27] E. Cerda and L. Mahadevan, Proc. R. Soc. A **461**, 671 (2005).
[28] T. A. Witten, Rev. Mod. Phys. **79**, 643 (2007).
[29] E. Infeld and G. Rowlands, *Nonlinear Waves, Solitons, and Chaos*, 2nd edition (Cambridge University Press, Cambridge, 2000).
[30] A. C. Newell, *Solitons in Mathematics and Physics* (Society for Industrial and Applied Mathematics, Philadelphia, 1985).
[31] F. Gesztesy and H. Holden, *Soliton Equations and Their Algebro-Geometric Solutions* (Cambridge University Press, Cambridge, 2003).